Japanese Journal of Ichthyology
Vol. 35, No. 4 1989

魚類学雑誌
35巻4号 1989年

Structure of the Air-Breathing Organs of a Swamp Mud Eel, *Monopterus cuchia*

Jyoti S. D. Munshi, George M. Hughes, Peter Gehr
and Ewald R. Weibel

(Received August 17, 1987)

Abstract The structure of the air-breathing organs of *Monopterus* (=*Amphipnous*) *cuchia* has been studied by using light, scanning and transmission electron microscopy and the morphological basis for buccopharyngeal respiration, aerial as well as aquatic has been established. Respiratory islets are well distributed over the surface of the buccopharynx, hypopharynx and branchial arches extending deep into the gill clefts but occupy only the anterior two-thirds of the air sacs, the remaining posterior one-third part seems to be non-respiratory in function and may serve as a reservoir for residual air. Arterioles penetrate deep into the epithelial region of air sacs and buccopharynx in spiral-like fashion to form the characteristic vascular papillae of the respiratory islets. In juvenile fish new respiratory islets develop in the non-vascular part of the air sac in between large older islets as sprout-like structures. The respiratory area, capillary loading, thickness of air-blood tissue barrier, and the diffusing capacity of the respiratory membrane of a 200 g fish were found to be 20 cm^2, 2.72 cm^3/m^2, 0.72×10^{-4} cm, and 0.00165 ml O_2/min/mmHg/kg, respectively.

The mud eel *Monopterus* (=*Amphipnous*) *cuchia* (Hamilton) belongs to the family Synbranchidae of the order Synbranchiformes (Rosen and Greenwood, 1976). It is an obligatory air-breather, which inhabits holes and crevices in the muddy banks of swamps, lakes, ponds and slowly running rivers containing fresh and brackish waters in the Indian sub-continent and Burma (Hora, 1935). The gross morphology (Munshi and Singh, 1968) and fine structure of the air-breathing organs of this species (Hughes and Munshi, 1973a; Munshi, 1976) and its vascular supply (Rosen and Greenwood, 1976; Satchell, 1976) have been studied.

In some earlier works on morphometry of the air-breathing organs the measurements of air-sacs were made taking into consideration only of their gross surface although the presence of non-respiratory and respiratory areas has been appreciated in many such species (Hughes et al., 1974a, b). In the respiratory regions there are quite extensive non-respiratory "Lanes" which would, therefore, reduce the overall values for respiratory surface (Hughes and Munshi, 1978). In addition, however, the respiratory islets themselves are often folded and this, together with the marked curvature of individual papillae would increase the surface area relative to that obtained by simple projection. In the morphometric study discussed here a new model has been adopted which takes these factors into account and has led to a modification in the previously published values for this species.

A detailed study of the structure of vascular papillae of the respiratory islets and morphometry of the air-breathing organs of *M. cuchia* was undertaken.

Materials and methods

Ten specimens of *Monopterus cuchia*, body weight 100–300 g and total length 550–700 mm, were transported by air from Calcutta, India to Bern, Switzerland and were kept in an aquarium at 25°C in the Department of Anatomy, University of Bern. They were fed with sheep liver and heart. Several specimens were anaesthetised in MS 222 (1 g/500 ml) and fixation was done by vascular perfusion. Compressed air was fed into the air sacs at a pressure of 20 cm H_2O and a cannula inserted into the bulbus arteriosus and perfusion initiated with oxygenated physiological saline (0.9% NaCl) containing 2500 IU heparin/litre. Perfusion was subsequently continued with a 2.5% glutaraldehyde solution in 0.03 molar potassium phosphate buffer (pH 7.4, 500 mil-

liosm.). Tissue samples were taken from the air sac, gill region, hypopharynx and buccopharynx following the glutaraldehyde perfusion. Tissue blocks were post-fixed in 1% osmium tetraoxide solution (pH 7.4, 350 millosm.), stained in a 0.05 molar uranyl acetate solution (pH 5, 350 milliosm.) dehydrated in a graded series of ethanols and finally embedded in epon for transmission electron microscopy (TEM). Post-fixation and staining were performed by perfusion and tissue samples removed from the air sacs and gills, dehydrated and embedded. Some samples were critical point dried with CO_2 after dehydration and sputtered with gold (50–60 nm) for scanning electron microscopy (SEM). Respiratory organs of a few mud eels were fixed, following anaesthesia by installation of 2.5% potassium phosphate buffered glutaraldehyde solution (pH 7.4, 350 milliosm.) through the mouth. Although attempts were made to seal the opercular slits some fluid was constantly leaking out which resulted in the pressure head varying between 15 and 55 cm H_2O. The fish was then kept submerged in the same glutaraldehyde solution for 3 hours. Afterwards tissue samples were taken from the same positions and processed for TEM and SEM as described above. In order to preserve the mucus lining of the respiratory surface, the anaesthetised fish was decapitated and the cranial portion of the head sectioned in a sagittal plane. The two halves were then submerged in glutaraldehyde to which ruthenium red (Ruthenium hexamine trichloride-RHT: Johnson Mathey Chemicals) was added at a concentration of 0.7% (final pH 7.1). Tissue samples were then taken from the same positions and post-fixed in OsO_4 (see above) to which 0.7% RHT was added. No block contrasting was performed; samples were directly dehydrated and embedded as above.

Gills and air sacs of juvenile fishes of 30–40 g were also fixed in 2.5% glutaraldehyde and post-fixed in 1% OsO_4 in phosphate buffer at pH 7.4 in Bhagalpur and were studied at Bristol.

Calculation of diffusing capacity: Diffusing capacity of the respiratory membrane was calculated using basically the same method as that employed for the mammalian lung (Weibel, 1979), which has previously been applied to the lungfish, *Lepidosiren* (Hughes and Weibel, 1976). The overall diffusing capacity (D_L) comprises the sum of the diffusing capacities of the different components as given below:

$$1/D_L = 1/D_t + 1/D_p + 1/D_e + 1/D_{mu}$$

Where, D_t, D_p, D_e and D_{mu} are the diffusing capacities of the tissue, plasma, erythrocyte, and mucus components respectively. For each components the diffusing capacity was calculated using the relationship: $D = K \times S/\tau_h$, except for D_e which is the product of V_c with the reaction rate constant for blood, θ_{o_2} ($\theta_{o_2} = 0.5$ ml/min/mmHg$=1/3$rd of 1.5 (Gehr et al., 1981) according to $K_{e'}$ of Holland and Forster (1966).

In these calculations the Krogh permeation coefficient for oxygen was the same as that used for mammalian tissue ($K_1 = 3.3 \times 10^{-6}$ ml O_2/min/mmHg/m²/μm) but calculations were also made with the smaller K_2 (1.5×10^{-6} ml O_2/min/mmHg/m²/μm) used for other air-breathing fishes for comparative purposes.

Results

Morphology. The air sacs are specialized suprapharyngeal pouches which develop as dorsolateral extensions of the pharyngeal cavity on each side. Sagittal section of the head shows the extensions of the buccal cavity, buccopharynx, hypopharynx and the air sac (Fig. 1). The vascularized respiratory surface extends up to the gullet in the hypopharynx, which is a distinct chamber separated from the oesophagus. The distribution of the vascularized respiratory islets on the inner mucosal linings of the pharynx, hypopharynx, and air sacs is shown in Figs. 2, 4, and 10. No respiratory islets are present in the most posterior part of the air sac, which presumably serves as a reservoir for residual air. Its surface is covered by non-vascular epithelium with many chromatophores.

Scanning electron microscopy. a) Buccopharynx: Under SEM the respiratory islets are seen separated from each other by deep furrows (Fig. 2). Fine slit-like clefts also divide each respiratory islet into several parts. The gill clefts between consecutive branchial arches are seen as narrow apertures lined by a membrane beset with many large and small islets (Figs. 3, 4).

The intra-epithelial capillaries arise from arteries and run in spiral-like fashion before opening into the veins (Fig. 3). They are covered over by a thin epithmeliu. The surface of epithelial cells

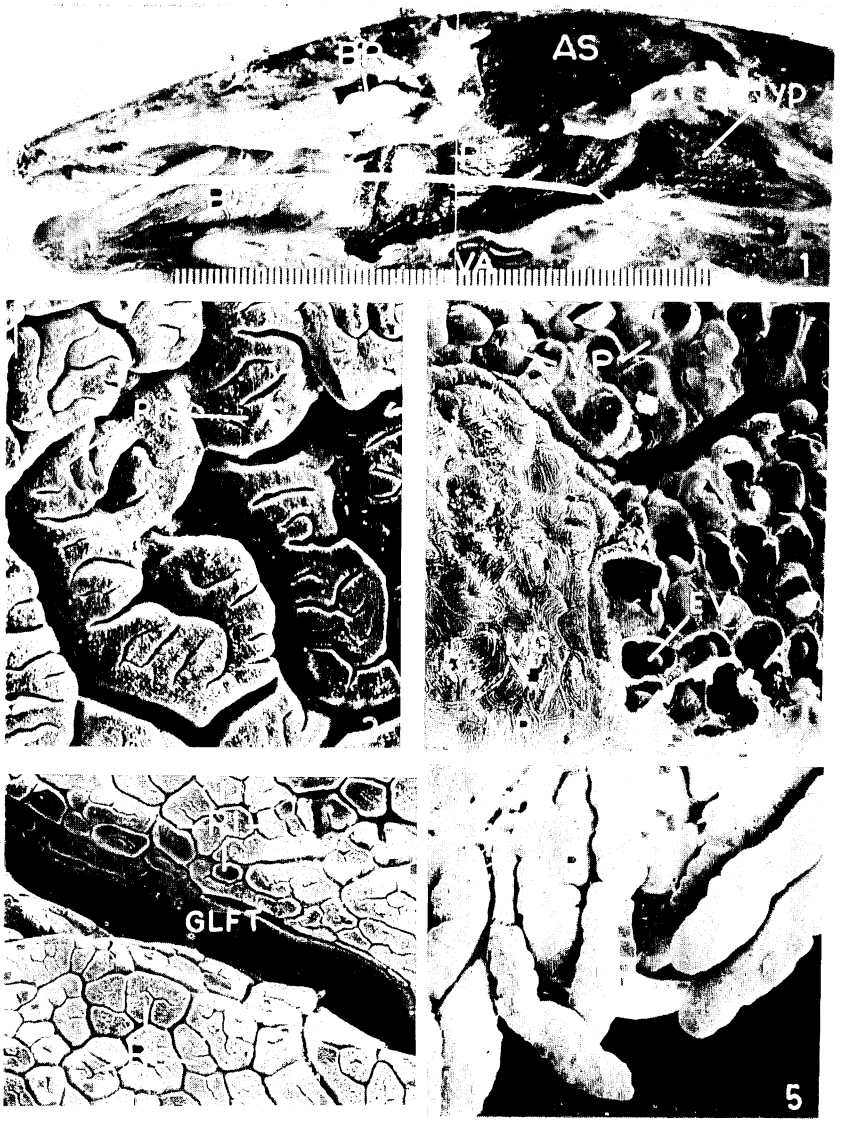

Fig. 1. Photograph of a dissection of the anterior region of *Monopterus cuchia*. White thread inserted to show the direction of flow of ventilating water. ×2. B, buccal cavity; Ph, pharynx; Hyp, hypopharynx; AS, air sac; GS, gill slit; VA, ventral aorta; BR, brain.

Fig. 2. SEM photomicrograph of buccopharyngeal region. Many small respiratory papillae are visible. ×50. RI, respiratory islet.

Fig. 3. Higher magnification of buccopharyngeal region showing microridged surface of non-vascular areas with openings of mucous glands and vascular region of islets with burst open vascular papillae and exposed endothelial valves. ×1000. MR, microridge; MG, mucous gland; EV, endothelial valve; VP, vascular papilla.

Fig. 4. SEM of pharynx showing cleft between successive arches. ×33. GLFT, gill cleft; RI, respiratory islet.

Fig. 5. SEM of second branchial arch showing intertwining gill filaments (GF). Note the slit-like pores near the base of the filaments representing the openings of interlamellar space. ×52. ILP, interlamellar pore.

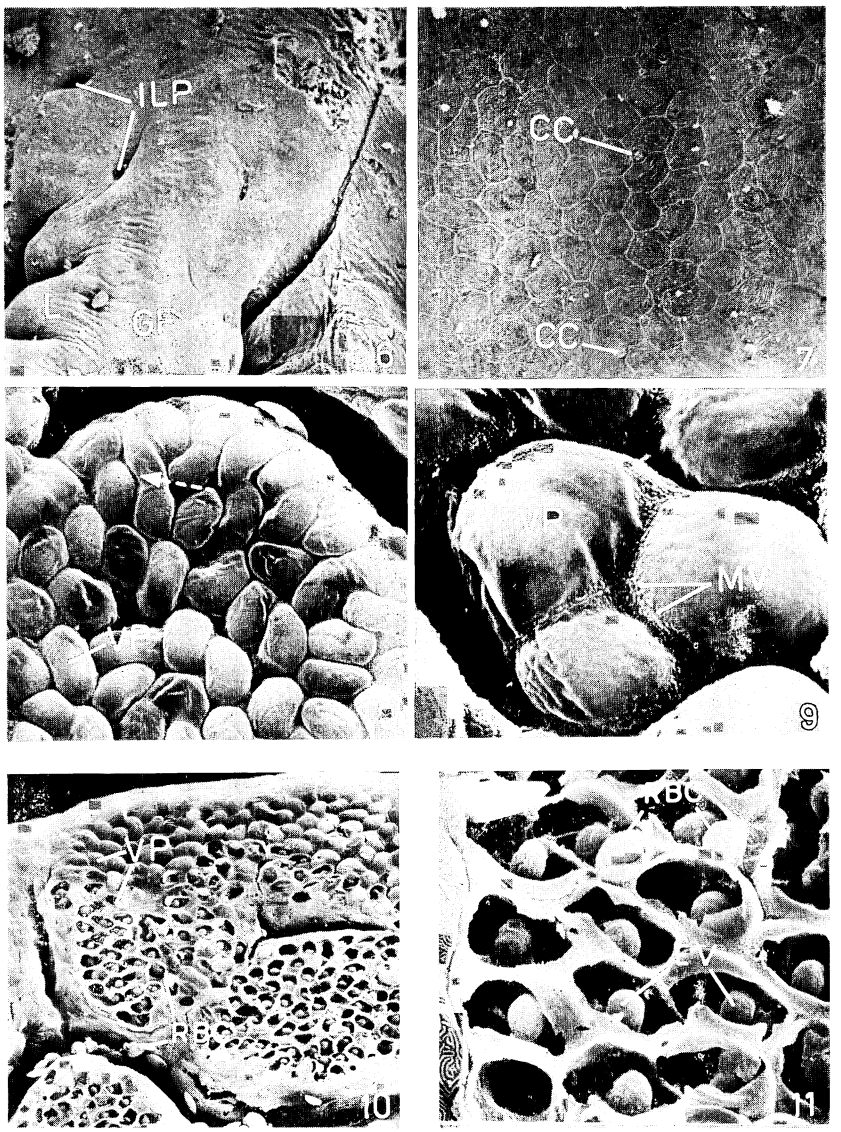

Fig. 6. SEM of a gill filament (GF) showing the lobules of budlike secondary lamellae (L) and slit-like pores of interlamellar space (ILP). ×216.

Fig. 7. Higher magnification of surface of a gill filament showing microridged epithelial cells and chloride cells (CC). ×1,094.

Fig. 8. SEM of a pharyngeal respiratory islet, showing the structure and formation of respiratory papillae (VP) of the blood capillaries. Note the orientation and spiral course of the capillaries (broken arrow). ×1,000.

Fig. 9. High power view of a group of respiratory papillae (VP) of the pharynx with their top smooth surface and microvilli (MV) at their bases near cell boundaries. Note the folds (=wrinkles) on the surface of the tough respiratory membrane. ×3,800.

Fig. 10. SEM of respiratory islets of hypopharynx, showing some of the ruptured papillae (VP) with scattered red blood corpuscles (RBC) in furrows between the islets. ×410.

Fig. 11. High power view of part of Fig. 10 showing the inner structure of respiratory vascular papillae with their characteristic endothelial valve (EV). Each valve forms the fulcrum-base of the vascular papilla leading its afferent pathway to the efferent side. ×2,000. RBC, red blood corpuscle.

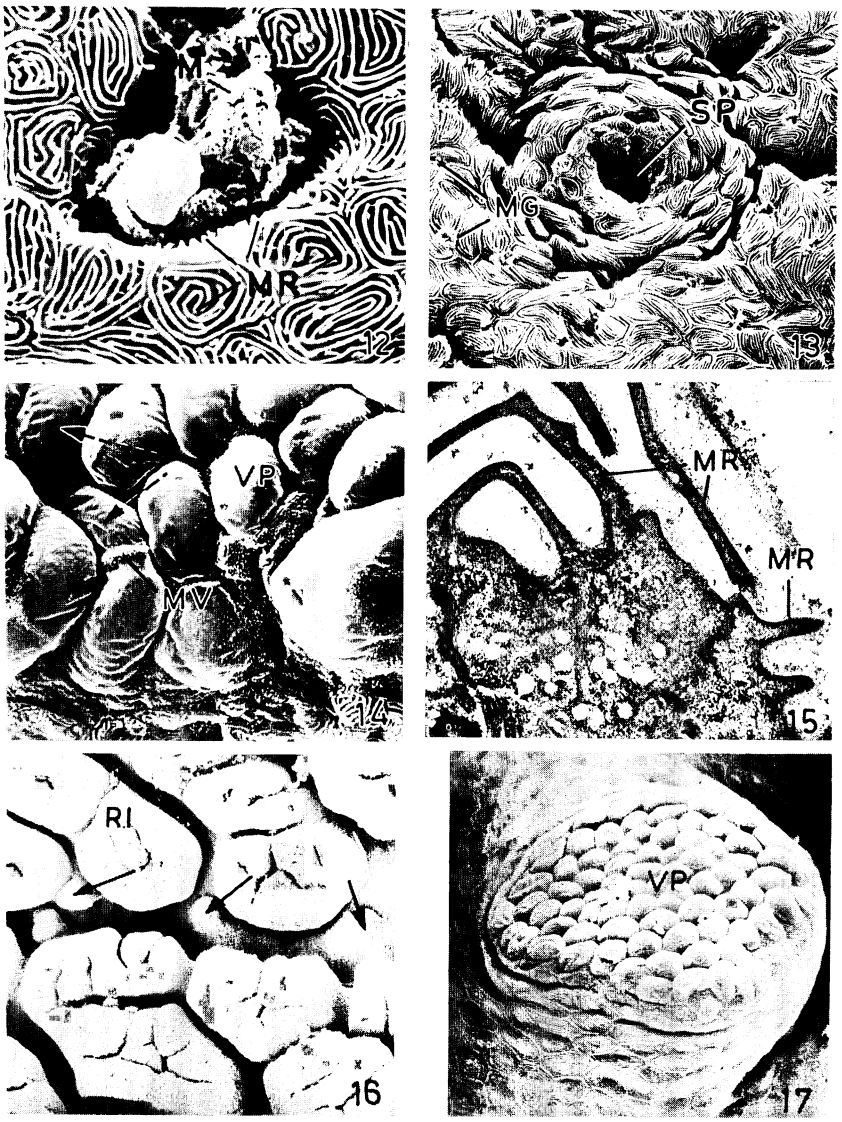

Fig. 12. High power view of non-respiratory 'lane' surface between the pharyngeal islets showing *micro*-ridged epithelial cells (MR) and a large pit containing mucus (M) and debris. Note the height of the ridges at the margin of the pit. ×4,200.

Fig. 13. Low power view of a sensory pit (SP) found in the non-vascular area of the air sac. Note openings of the mucous glands (MG). ×1,000.

Fig. 14. High power view of a respiratory islet of air sac showing the structure of respiratory papillae (VP). Note the spiral/wave-like course of the blood capillaries which form the respiratory vacsular papillae (VP) and microvilli (MV) of the epithelial cell junctions. ×2,000.

Fig. 15. TEM of a section of non-respiratory area of air sac cutting across the epithelial surface showing furrow formed by microridges (MR) containing mucus. Also note the height and thickness of microridges. ×15,300.

Fig. 16. SEM (low power) of air sac of a juvenile fish showing three developing respiratory islets (arrow) in the lane between the mature respiratory islets (RI). ×95.

Fig. 17. Higher magnification of above showing the structure of a developing islet containing a basketful of respiratory vascular papillae (VP). ×936.

covering the vascular papillae is rather smooth, the microvilli being present at their margins near cell junctions (Fig. 9). In non-vascular 'lanes' between the islets many pits are seen containing mucus and some sort of debris; they are lined by microridged epithelial cells (Fig. 12).

b) Hypopharynx: Even the hypopharynx which leads into the oesophagus is respiratory in function. Where the delicate tissue barrier is peeled off, the inner structure of the vascular papillae is exposed (Figs. 10, 11). The "cells" of the vascular papillae of the respiratory islet give a honeycomb appearance (Fig. 10). The endothelial cells with their prominent round nuclei characterize the "cell" structures. In all such "cells" the endothelial cells are found attached to the floor of the blood capillary, forming an axis over which the blood corpuscles move from one space to another (Fig. 11).

c) Gills: The second branchial arch bears a few fingershaped filaments (Fig. 5). There is no differentiation of secondary lamellae which are represented by short elevated protuberances on the margins of the filaments (Fig. 6). Near the base of the gill filaments where they remain fused with the branchial arch, holes or slit-like apertures are found (Fig. 6), which represent interlamellar spaces. The surface of the filaments is covered over by microridged epithelial cells (Fig. 7). In between these microridged cells are found small triangular-shaped microvilli-bearing areas which represent the apical parts of the chloride cells (Fig. 7).

d) Air sac: i) Non-vascular area: About 1/3rd of the air sac, especially its dorso-posterior region seems to be non-respiratory in nature. This area is covered by microridged epithelial cells of varied configurations (Fig. 12). A chemoreceptor is seen in a pit bounded by small microridged cells (Fig. 13).

ii) Vascular respiratory surface: Under low magnification the folds of the sac are clearly visible (Fig. 13), along with the typical vascular respiratory islets of different dimensions and shapes (Figs. 14, 16). In the air sac micro air pockets have been detected which penetrate deep into the air sac wall.

iii) Development of respiratory islets: In juvenile fish, new respiratory islets with 75–80 vascular papillae develop in the non-vascular lanes of the air sac in between large older islets (Figs. 16, 17).

Light and transmission electron microscopy. In vertical sections of the air sac wall the vascular respiratory and glandular non-respiratory areas are clearly distinguishable (Fig. 18).

Non-respiratory area: The non-respiratory areas are composed of polyhedral epithelial cells of several layers. The surface is covered by microridged epithelial cells. When viewed by TEM the epithelial cells have well-spaced microridges on the surface and many ill-defined vesicles and polymorphic nuclei in the cytoplasm (Figs. 15, 18). In ruthenium red-treated preparations the darkly-stained thick mucus layer is seen both over the respiratory islets and non-respiratory surfaces. The unicellular mucous glands are restricted to the non-respiratory areas of the air sac (Fig. 18). They contain globules of mucus having dark osmiophilic granules. Each mucous gland opens to the outside in between the microridged cells.

Respiratory islets: The connective tissue layer of the air sac, which is equivalent to the dermal layer of skin, is formed of a matrix substance in which fibrocytes abound. The respiratory islets are formed of intra-epithelial blood capillaries which run in spiral-like fashion (Fig. 14). They are packed into the smallest area possible forming the respiratory islets. The endothelial cells with their characteristic round nuclei airse from the basal wall or floor of a blood capillary (arteriole) to form the valve-like axes of the vascular papillae, which get further support from tucked in epithelial cells (Fig. 19). The red blood corpuscles move over the endothelial complex so as to come into direct contact with the gas exchange surface. Many mitochondria are present in the basal cytoplasm of the endothelial cells. Flattened as well as round vesicles have been observed in large numbers in the cytoplasm of the endothelial cells. The endothelial lining of blood capillaries becomes very thin (0.4 μm) just below the thin basement membrane overlying the vascular papilla (Fig. 19). The air-blood tissue barrier is formed of three distinct layers namely, the thin outer epithelial cells (0.30 μm), the (transparent) basement membrane (0.06 μm) and the endothelial lining (0.4 μm) (Fig. 20). Microvilli are present only at the marginal areas of the vascular papillae. The supporting epithelial cells extend between the contiguous vascular papillae to form pillar-like structures (Fig. 18).

Morphometry. The respiratory membrane lin-